Egyptian Journal of Chemistry

http://ejchem.journals.ekb.eg/

Design, Spectroscopic Characterization, Thermal, 3D Molecular Modeling, XRD and in Vitro Antioxidant and Antimicrobial Screening of Novel N_2O_2 Tetradentate Schiff Base Metal Complexes

Hanaa A. El-Boraey[a], Azza A.Serag El-Din[b], Ohyla A. EL-Gammal[c]*

[a]*Department of Chemistry, Faculty of Science, Menoufia University, Shebin El- Kom, Egypt*

[b]*Department of Chemistry, the Regional Institute Joint of Medical and Chemical Analysis, Ministry of Health, Shebin El-Kom, Egypt*

[c]*Department of Pathology, University Hospital, Menoufia University, Shebin El- Kom, Egypt*

Abstract

In the present study, new Co(II), Ni(II) and Cu(II) complexes were synthesized from the reaction of tetradentate Schiff's base ligand (H2L)= (N, N'-(pyridine- 2,6- diyl) bis (2- (((Z)- (2- hydroxynaphthalen-1-yl) methylene) amino) benzamide that was synthesized via condensation of 2-amino-N-{2-[(2-amino-benzoylamino) pyridine]-benzamide} with 2-hydroxy-1-naphthaldehyde. The ligand and its metal (II) complexes were characterized by microanalyses, magnetic, spectral, powder X-ray diffraction (XRD) and thermal studies. An octahedral geometry has been proposed for [Co(L)(H2O)2].3H2O (1), [Ni(L)(H2O)2].1½H2O (2) and square planar for [Cu(L)](3) and [Cu(H2L)(OH)Br](4). EPR spectra of Cu(II) complexes are consistent with dx^2-y^2 ground state. 3D molecular modeling studies have been carried out for ligand and complex (1). Average crystallite size (D) and dislocation density (δ) were calculated from XRD. All compounds were screened for their in vitro antioxidant activity. The results showed that the ligand possesses excellent activity compared to the reference (Ascorbic acid) and complex (4) was the most potent one. Moreover, the current compounds were tested for their antimicrobial activity.

Keywords: Schiff's base ligand; 2-hydroxy-1-naphthaldehyde; spectral studies; molecular modeling; X-ray diffraction; antioxidant and antimicrobial activities.

1. Introduction

Acyclic ligands having nitrogen and oxygen donating atoms in their geometry can act as complexing agents for transition, s- and p- block, lanthanides and actinides metal ions [1-6]. A lot of interest has been paid to the compounds containing azomethine, Schiff's bases, because of their ease of synthesis and remarkable applications [4,7-9]. Imine group is significantly important for the biological activities of Schiff's base ligands and their metal complexes. Formation of stable Schiff's base metal complexes relying on properties of Schiff's base donor atoms as well as the properties of metal ion and on the coordinating ability of counter ions [1,2,7-10]. Large number of Schiff's base ligands and their complexes were studied for their wide range of pharmacological applications such as anticancer [11,12], antibacterial, antifungal, antiviral and other biological applications [7-9,13,14]. Besides the biological activity, photochromism and solid-state thermochromism are common in these compounds, leading to their application in material science fields such as display systems and optical memory devices and measurement of radiation intensity [15-17]. Other applications as in

*Corresponding author e-mail: ohyla55@yahoo.com (Ohyla A. El-Gammal)
Receive Date: 28 March 2021, Accept Date: 26 April 2021
DOI: 10.21608/EJCHEM.2021.69667.3539

electrocatalysis, inhibitors of corrosion [18-20], catalysts, in medicine which includes antibiotics, anti-inflammatory, antioxidant, antidiabetic as well as analgesic agents are reported [14,21,22]. Reactive oxygen species (ROS) and free radicals are important in the protection mechanism towards oxidative damage [14]. Researches have showed that compounds that may neutralize free radicals can be great interest in the prevention of some types of cancer [23]. On the other hand, Schiff's bases containing O-H groups on the aromatic ring are the most effective and potent antioxidants [23]. The Schiff's bases contain g (N) and (O) donor atoms possess important medicinal application [6,12]. Furthermore, the presence of 2-hydroxy-1-naphthaldehyde as precursor offers suitable binding sites for coordination with metal ions. So, this class of Schiff's bases may also behave as polydentate ligands. Tetradentate Schiff's base, that have two (N) and two (O) atoms possess an excellent mode of coordination with metal ions, so this type of Schiff's base have important studies [24]. In view of the interest and importance of these ligands, we have synthesis (N, N'- (pyridine- 2,6- diyl) bis (2- (((Z)- (2- hydroxynaphthalen-1-yl) methylene) amino) benzamide ligand and some of its transition metal(II) complexes. The compounds had been assigned by analytical and spectroscopic methods as microanalyses, spectral, 3D molecular modeling, powder X-ray diffraction, magnetic susceptibilities, thermal technique and molar conductance. Moreover, the in vitro antioxidant activity and in vitro antimicrobial activity against Gram-positive bacteria as (Staphylococcus aureus) and Gram-negative bacteria as (Escherichia coli) and antifungal activity as (Aspergillus flavus and Candida albicans) were studied.

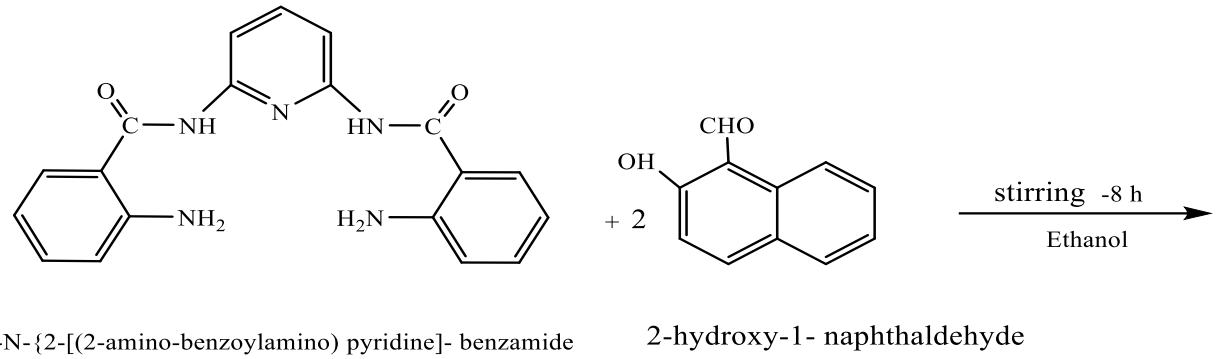

2-amino-N-{2-[(2-amino-benzoylamino) pyridine]- benzamide

2-hydroxy-1- naphthaldehyde

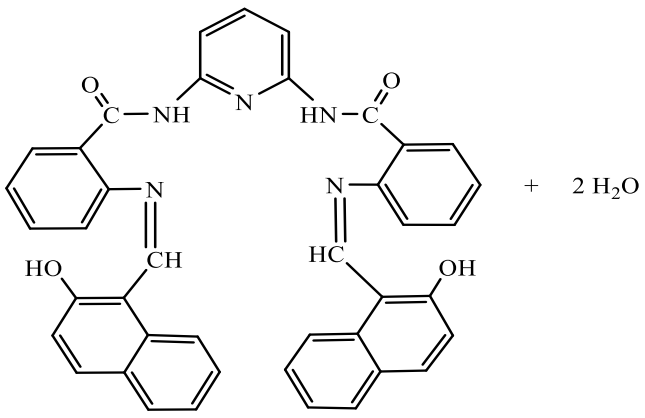

H_2L

Scheme 1: Synthetic route for the preparation of the Schiff base ligand.

2. Experimental section

2.1. Reagents and physical instruments

All used chemicals were of AnalaR grade and purchased from Sigma–Aldrich and Fluka. Metal(II) salts and used solvents (E. Merck) were commercially available as pure samples and used as it is. Microanalyses, metal and halide ions were determined using standard methods [25,26]. FT-IR, ^{1}H NMR spectrum, Electron Impact (EI) and (ESI-MS), UV-Visible absorption and electron paramagnetic resonance (EPR) spectra, molar conductivity, magnetic susceptibilities, thermal analysis (TG/DTG) and X- ray powder diffraction analyses were all performed as described in the literature [8, 27].

2.2. Synthesis of Schiff base ligand (H2L)

The ligand has been synthesized as shown in Scheme 1. (2-amino-N-{2-[(2-aminobenzoylamino) pyridine]-benzamide) (2.89 mmol, 1gm) in ethanol (20 mL) was added gradually to 2-hydroxy-1-naphthaldehyde (5.74 mmol, 0.99 gm) in the same solvent. The resultant mixture was stirred at room temperature for about 8 h. The shiny orange solid product obtained was removed and washed by cold ethanol and dried over P_4O_{10} (Melting point = 174 ^{o}C) [27].

2.3. Synthesis of the metal complexes

Co(II), Ni(II) and Cu(II) complexes **(1-4)** were synthesized using the subsequent preferred technique. To a suspension of the ligand (H_2L) (0.5 gm) in ethanol (20 mL), a solution of different metal salt {$CoCl_2.6H_2O$ (0.18 gm), $Ni(NO_3)_2.6H_2O$ (0.22 gm), $Cu(ClO_4)_2.6H_2O$ (0.28 gm) or $CuBr_2$ (0.17 gm)} in 20 mL ethanol was added in molar ratio 1:1 (Ligand: Metal) for complexes (**1**), **(2)**, **(3)** and **(4)**, respectively. The reaction mixture was stirred under reflux for 6 h. The formed precipitate was gathered by filtration, washing by cold ethanol followed by drying over P_4O_{10}.

2.4. 3D Molecular modeling studies

The 3D molecular modeling studies using Molecular Mechanics, MM plus force field for ligand and its Co(II) complex (**1**) were carried out on Chem 3D 15.0 version. The version has wide applications in coordination chemistry through calculation of parameters such as bond lengths and bond angles.

2.5. Biological tests

2.5.1. In vitro antioxidant studies

The antioxidant activity of synthesized ligand and its metal complexes was tested at National Centre Institute, Egypt by the use of the stable free radical 2,2-diphenyl-1-picrylhydrazyl (DPPH). The free radical scavenging effects of the present compounds had been evaluated by Blois method and Ascorbic acid was used as standard [28,29]. The percentage of free radical scavenging activity (% inhibition) was evaluated by using the equation:

$$\% \text{ Inhibition} = [(A_c - A_s)/A_c)] \times 100$$

Where A_c is the absorbance of DPPH solution without sample, A_s is the absorbance of sample solution with DPPH.

2.5.2. In vitro antimicrobial studies

Antibacterial and antifungal activities of the tested compounds have been examined in vitro against the bacteria species, Gram- positive strain as Staphylococcus aureus (ATCC No. 12600) and Gram-negative strain as Escherichia coli (ATCC No, 11775) and fungal strain as Aspergillus flavus and Candida albicans (ATCC No. 7102) with helping the modified Kirby-Bauer disc diffusion approach [30]. Standard discs of Ampicillin (antibacterial drug) and Amphotericin B (antifungal drug) used as positive controls for antimicrobial activity. The organisms had been grown on Meuller-Hinton agar that is carefully tested for composition and pH in petri plates. The activity of tested samples was studied at concentration (10 mg mL^{-1}) in DMSO as controlling solvent and soaked in paper disks (Schleicher & Schuell, Spain) with a diameter of 8.0 mm, the disks have been placed on formerly seeded plates. Plates inoculated with filamentous fungi at (25 ^{o}C for 48 h) and (30 ^{o}C for 24-48 h) for Aspergillus flavus and Candida albicans (ATCC No.7102), respectively. Gram positive bacteria strain as Staphylococcus aureus (ATCC No. 12600) and Gram- negative bacteria strain as Escherichia coli (ATCC No.11775) were incubated at 35-37 ^{o}C for 24-48 h. The diameter of "inhibition Zone" round every disc was measured.

3. Results and discussion

3.1. Physical properties

The purity of current ligand and its complexes has been tested with the aid of TLC. All the metal complexes are non-hygroscopic and stable. Table 1 shows color, elemental analyses and molar conductivity of the metal complexes. The microanalyses data of the complexes **(1-4)** suggest that the complexes are formed in 1M:1L molar ratio.

All complexes are insoluble in most common organic solvents but freely soluble in hot DMSO or DMF solvent. So, the crystals of all complexes could not be grown. Thus, X-ray crystallography is not possible. The low values of molar conductivity of complexes (11- 22 Ω^{-1} cm^2 mol^{-1}) in 10^{-3} M DMSO solvent indicate that they are non-electrolyte [31].

3.2. Elucidation of the ligand structure

3.2.1. FT-IR spectrum

The FT-IR absorptions data of the Schiff's base ligand are listed in Table 2. The intense band at 1622 cm^{-1} is assigned to the (–CH=N) stretching frequency. Additionally, IR spectrum of the ligand exhibits a broad band at 3436 cm^{-1}, assigning to the stretching vibration of naphtholic υ(OH) group [12, 32].

3.2.2. ^{1}H NMR and mass spectral studies of the ligand

The ^{1}H NMR was carried out to obtain an insight into the formed ligand structure. The ^{1}H NMR spectrum of current ligand was performed in DMSO-d_6 solution (Fig. 1). The spectrum exhibits a multiple signal at δ (6.910-8.681 ppm) due to protons of aromatic and pyridine rings. Also, the spectrum depicts signals at δ (8.7002, 9.001 and 9.601 ppm) due to (2H, –CH=N–), (2H, –CO–NH–) and (2H, –OH) protons, respectively [33]. The electron impact mass spectrum of the ligand (Fig. 2) displays observed peak at *m/z* = 655 *amu* (M) corresponding to the ligand moiety ($C_{41}H_{29}N_5O_4$, atomic mass *m/z* = 655). Additional peaks in the range *m/z* = 75 $[C_6H_4]^+$, 143 $[C_{10}H_7O]^+$, 246 $[C_{17}H_{12}NO]^+$, 381 $[C_{23}H_{17}N_4O_2]^+$, 485 $[C_{30}H_{21}NO_3]^+$, may be assigned to different fragments. Thus, the ^{1}H NMR result and (EI) mass spectrum of the ligand support the proposed structure.

3.3. Characterization of the metal complexes

3.3.1. Electrospray mass spectra (ESI-MS) for the complexes

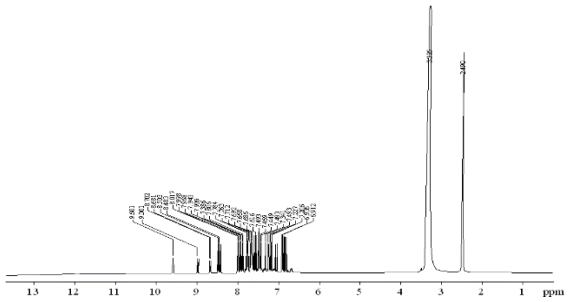

Fig. 1: Nuclear magnetic resonance spectrum of H_2L.

ESI - mass spectra of $[Co(L)(H_2O)_2].3H_2O$ **(1)** and $[Cu(H_2L)(OH)Br]$ (**4**) complexes were carried out in DMSO-d_6 solvent (Fig. 2). The spectra show signals coincide and confirm the proposed formulae, the observed molecular ion peaks at *m/z* 803, 816 *amu* (calculated M= 802.5, 815.5 *amu*, respectively) coincide with their formulae weight. Also, the spectra of the complexes **(1,4)** showed other fragment ion at *m/z* values like at: Calc/Found 63/63 $[C_5H_3]^+$, 77/77$[C_5H_3N]^+$, 163/163 $[M\text{-}C_{34}H_{32}N_2O_7Co]^+$, 420.5/418.5$[M\text{-}(C_{22}H_{22}O_6)\text{-}2H^+]^+$,748/747[M-(3$H_2O$-$H^+$)]$^+$ for complex (**1**) and fragment ion at *m/z* 76/76$[C_6H_4]^+$,100/100$[C_7H_4O]^+$,274/274$[C_{18}H_{12}NO_2^+$, 417/417$[M\text{-}(C_{23}H_{18}N_4O_3)]^+$, 708.5/708 $[M\text{-}C_5H_5N_3]^+$ for complex (**4**). The observed data confirmed the suggested structures.

Table 1: Microanalyses and physical data for the compounds

No.	Compound	Color	Empirical formula	Yield (%)	Microanalyses Calc./ Found (%)					$(\Lambda_m)^a$
					C	H	N	M	Br	
	H_2L	Orange	$C_{41}H_{29}N_5O_4$	65	75.11/75.94	4.42/4.38	10.68/10.15	-	-	-
1	$[Co(L)(H_2O)_2].3H_2O$	Brown	$C_{41}H_{37}N_5O_9Co$	64	61.30/60.80	4.61/4.62	8.72/9.00	7.41/6.89	-	22
2	$[Ni(L)(H_2O)_2].1½H_2O$	Pale brown	$C_{41}H_{34}N_5O_{7.5}Ni$	86	63.48/64.61	4.38/4.66	9.03/8.75	7.61/7.2	-	20
3	[Cu(L)]	Dark brown	$C_{41}H_{27}N_5O_4Cu$	76	68.66/68.82	3.76/4.05	9.76/9.10	8.86/9.2	-	11
4	$[Cu(H_2L)(OH)Br]$	Dark brown	$C_{41}H_{30}N_5O_5BrCu$	77	60.33/59.86	3.67/3.67	8.58/8.48	7.78/8.0	9.80/10.2	17

[a]: Ω^{-1} cm^2 mol^{-1} DMSO solution (10^{-3}M).

Table 2: Important IR spectral bands (cm^{-1})[a], UV-Visible electronic data ($\lambda_{max,}$ nm) and magnetic moment values (μ_{eff} B.M.) of the investigated compounds.

No.	Compound	$\nu_{(OH/H2O)}$	ν(C=N)	$\nu_{(C-O)}$	$\nu_{(M-O)}$	$\nu_{(M-N)}$	λ_{max} (Nujol mulls, nm)		μ_{eff}
							(d-d Transition)	Intra-ligand and CT ban	(B..M)
	H_2L	3436(b)	1622(s)	1232(m)	-	-	-	487, 320, 220	-
1	$[Co(L)(H_2O)_2].3H_2O$	3421(b)	1623(m)	1255(m)	619(w)	582(w)	695,510	360, 320, 240	5.23
2	$[Ni(L)(H_2O)_2].1½H_2O$	3406 (b)	1618(s)	1253(m)	521(w)	459(w)	665, 530	476, 344, 230	3.40
3	[Cu(L)]	-	1622(s)	1253(m)	490(w)	418(m)	680, 520	427, 323, 229	2.26
4	$[Cu(H_2L)(OH)Br]$	3452(b)	1617(m)	1232(w)	521(m)	456(s)	700, 520	476, 347, 251	2.00

[a]: s, strong; m, medium; w, weak; b, broad; ν, stretching

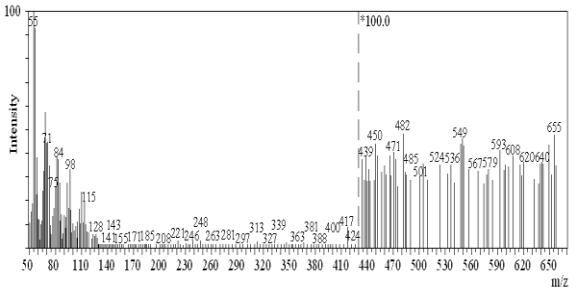

Fig. 2: EI spectrum of H2L ligand.

3.3.2. IR spectra and mode of bonding

The infrared spectrum of free ligand is compared with that of its metal complexes, to determine the mode of its bonding to the metal(II) ion, the band of the imine (–CH=N) of the free ligand was shifted to 1632-1617 cm^{-1} (Table 2) and the naphtholic υ(C-O) band is shifted from 1232 to 1255–1253 cm^{-1}, indicating the coordination of the ligand to the metal(II) ion *via* N of imine group and O of deprotonated naphtholic atoms. This is in consistence with the appearance of two new bands in far infrared regions around 619-490 and 582-418 cm^{-1}, assigning to υ(M-O) and υ(M-N) chelation modes, respectively [12, 32, 34]. From the IR spectral data, we can concluded that the current ligand coordinated through the nitrogen of imine groups and naphtholic oxygens and behaves as tetradentate one, except for Cu(II) complex (**4)** in which the ligand coordinates to two imine nitrogen's only. Thus, the IR spectral data offer appropriate evidences for the mode of coordination of the Schiff's base ligand.

3.3.3. Electronic spectra and magnetic measurements

The UV-Visible spectral bands of all compounds and the magnetic moments measurements can be provided data to establish their geometry. Nujol mull (λ_{max}, nm) electronic absorptions and effective magnetic moment (μ_{eff} B.M.) values at RT are tabulated (Table 2). All compounds exhibit the high energy bands in the range 251–220, 347–315 and 487–360 nm ascribing to π→π*, n→π* and charge transfer (CT) transitions, respectively.

3.3.4. Electronic spectra

The UV-Visible spectrum of the Co(II) complex $[Co(L)(H_2O)_2].3H_2O$ (**1)** displays d-d bands at 695 and 520 nm, assigning to the $^4T_{1g}$ (F)→$^4A_{2g}$ (F) (ν_1) and $^4T_{1g}$(F)→$^4T_{1g}$(P)(ν_2) transitions, respectively suggesting six coordinated Co(II) ion [35, 36]. While, the electronic absorption spectrum of Ni(II) complex $[Ni(L)(H_2O)_2].1½H_2O$ **(2)** displays two recognizable d-d bands at 665 and 530 nm, attributable to the $^3A_{2g}$(F)→$^3T_{1g}$(F) and $^3A_{2g}$(F)→$^3T_{1g}$(P) transitions, respectively, the presence of these bands are consistent with those expected for octahedral Ni(II) ion [37, 38]. The electronic absorption spectra of Cu(II) complexes (**3)** and **(4**) reveal two bands at 700-680, 520 nm assigning to $^2B_{1g}$→$^2B_{2g}$ and $^2B_{1g}$→ $^2E_{1g}$ transitions, respectively consistent with square planar geometry around Cu(II) ion [39-41].

3.3.5. Magnetic measurements

Table 2 shows the measured magnetic moment values for the complexes (**1-4**) at RT. For Co(II) complex (**1)**, the RT μ_{eff} equals 5.23 B.M. It is notice that, μ_{eff} value is higher than experimental observed spin only of high-spin octahedral cobalt(II) complexes. This deviation can be attributed to spin orbit coupling [42]. The μ_{eff} value of the Ni(II) complex (**2**) is 3.4 B.M.

gives adequate support to six coordination around the Ni(II) ion [34]. The μ_{eff} values for Cu(II) complexes **(3,4)** are 2.26, 2.00 B.M., respectively,

confirming their mononuclear nature. Moreover, the μ_{eff} value obtained for Cu(II) complexes (**3), (4**) (Table 2) is characteristic for the square planar geometry of the Cu(II) complexes [43].

3.3.6. EPR spectroscopic studies

The EPR solid state spectrum of Cu(II) complexes **(3,4)** provides information about the environment of the metal ion **(**Fig. 3**)**. The complexes give axial spectra, from calculated data it is seen that $g_{//}$ = 2.1764, 2.2187 and $g_{\perp}$ = 2.0335, 2. The $g_{//}$ values are <2.3 indicating covalent character for Cu-ligand bond [44, 45]. The exchange coupling interaction between two copper centres is calculated by Hathaway expression $G = g_{//}$ -2.0023/ $g_{\perp}$ -2.0023 [46]. Value of G > 4.0, clarifying that there is negligible exchange interaction between copper centres in the solid state. The obtained G value is 6.93, 4.145 for complexes **(3,4)**, respectively, implying no exchange interaction [24]. The empirical factor $f = g_{//}/A_{//}$, is an index of tetragonal distortion. The values lower than 135 cm^{-1} are observed for square planar structures while values greater than 150 cm^{-1} for tetrahedrally distorted complexes [24,42]. The calculated empirical factor f value for complexes **(3, 4)** equals 116.77, 120 cm^{-1}, respectively confirming the square planar geometry.

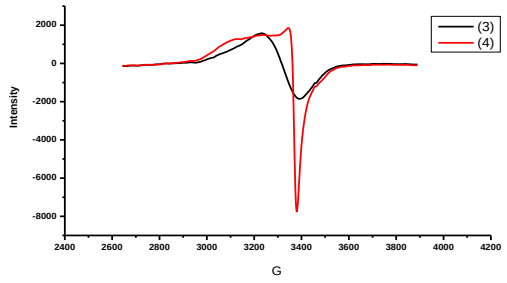

Fig. 3: EPR spectra for Cu(II) complexes (**3,4**).

3.4. Thermal studies

The thermogravimetric (TG/DTG) analysis is very important technique used to assess the stability of compounds and confirm their geometry structure. (TG/DTG) results are recorded in Table 3. The thermal studies of the reported compounds show good agreement with the suggested theoretical formulae obtained from analytical and spectral data [35, 47].

3.4.1. Ligand

The TGA curve of the ligand shows two successive decomposition steps within 174-799 ºC range. The first step of decomposition occurs within the 174-512 ºC range with endothermic DTG peaks at 307, 414 ºC which corresponds to mass loss of different parts of ligand (naphthol, azomethine, benzene, two amide group and pyridine) moieties with mass loss of 62.56 %(Calc. = 62.44%). The second step of decomposition occurred within 512-799 ºC range, with DTG peaks at 576, 645 ºC with mass loss of (Calc./Found%: 37.56/37.44), which is due to removal of the rest of the ligand (benzene and naphthol) moieties.

3.4.2. Cobalt(II) chelate

The TGA thermogram of cobalt(II) complex (**1**) (Fig. 4) shows mass loss (Calc./Found%: 6.72/6.60) with strong DTG peak at 44 ºC, is attributed to removal of three molecules of hydration water within 28-116 ºC range. This process was followed by steady part from 116 to 220 ºC. The thermogram also shows two stages of decomposition within temperature range 220-488 ºC and 488-799 ºC, the first stage with mass loss of (Calc/Found %:25.56/24.99) with DTG peaks at 250, 299, 339 ºC corresponds to the loss of two coordinated water molecules together with naphthol and azomethine moieties. The second decomposition step occurred within temperature range 488-799 ºC with mass loss of (Calc./Found%:49.34/49.41) with broad DTG peak at 552 ºC corresponds to the elimination of the rest of the ligand {benzene ring, two amides, pyridine, azomethine and naphthol} moieties, leaving metal oxide CoO contaminated with carbon (Calc./Found%: 18.40/19.00) as final residue [35, 36].

3.4.3. Nickel(II) chelate

The TGA curve of nickel(II) complex (**2**) (Fig. 4) displays mass loss (Calc./Found%: 3.48/3.28) with DTG peak at 54 ºC which corresponds to loss of one and half molecule of lattice water within the temperature range 30-110 ºC. The thermogram also shows two stages of decomposition within temperature range 232-432 ºC and 432-650 ºC. The first decomposition step with mass loss (Calc./Found %: 36.12/36.43) with DTG peaks at 293,355,400 ºC corresponds to loss of two coordinated water molecules together with loss of different parts of ligand {naphthol, azomethine and benzene ring} moieties as shown in Table 3. The second step with mass loss (Calc./Found%: 52.79/52.51) corresponds to the elimination of the rest of the ligand {two amide groups, pyridine ring, benzene ring azomethine and naphthol} moieties. The TG thermogram of the complex ended with the formation of Ni as final

residue (Calc./Found %: 7.61/7.78) [42].

3.4.4. Copper(II) chelates

The steady part of the TGA thermograms of copper(II) complexes (**3)** and **(4**) till 193 and 222 ºC, respectively, indicates the absence of any outside solvent (Fig. 4**)**. The Cu(II) complex **(3)** gradually decomposed in two stages. The first decomposition step with mass loss (Calc./Found %: 50.94/50.0) with DTG peaks at 325,387,468 ºC is due to loss of ligand (naphthol, azomethine, benzene, amide group and pyridine) moieties in the temperature range 193-576 ºC. The second decomposition step with mass loss (Calc./Found%:40.20/41.30) in the temperature range 576-799 ºC with broad DTG peak at 611 ºC, corresponds to the elimination of the rest of the ligand (amide group, benzene ring, azomethine and naphthol) moieties. The TG thermogram of copper(II) complex **(4)** (Fig. 4**)** also gradually decomposed in two stage, the first decomposition stage shows mass loss (Calc./Found %: 32.74/ 32.94) in 222- 520 ºC range with DTG peaks at 305, 397, 424 ºC which is related to removal of half bromine molecule and hydroxyl group, azomethine, naphthol moieties. The second stage shows mass loss (Calc./Found %:59.47/60.01) with broad DTG peak at 649ºC in the temperature range 520-750 ºC corresponds to the elimination of the rest of the ligand. For both complexes (**3)** and **(4**) the TG thermogram ended with the formation of Cu metal as final residue [48]. The remaining residue was reported and identify by IR spectroscopy for all complexes.

On the other hand, if the initial temperature of the decomposition (*Td*) (Table 3) peak is taken as a measure of the thermal stability of the current compounds, some observations and conclusions can be summarized as follows:

- All complexes are thermally stable than their metal free ligand.
- The thermal stability of the octahedral Ni(II) complex **(2)** (232 ºC) is more than the corresponding isostructural Co(II) complex **(1)** (220 ºC) which may be due to the higher electronegativity and lower ionic radii of Ni(II) ion than that of Co(II) ion. As the ionic radii decreases (higher charge/radius ratio) the thermal stability increases which can be explained by the higher metal to ligand interaction [49].
- The square planar Cu(II) complex (**4)** displays different thermal stability than the square planar Cu(II) complex (**3**), this may be due to their different groups around Cu(II) ions. The structure of Cu(II) complex (**4**) may be stabilized through hydrogen bonding formed between the hydroxyl and azomethine groups together with the presence of the bromide anion which plays significant role in the thermal stability.
- The difference in the thermal stability between the isostructural octahedral Co(II), Ni(II) and the square planar Cu(II) complexes can be explained from the coordination number view point.
- The thermal analysis is compatible with the formulae of the complexes suggested from spectral and analytical data.

3.5. 3D Molecular modelling studies

The geometry of the ligand H_2L and its $[Co(L)(H_2O)_2].3H_2O$ complex (**1**) was optimized by Chem 3D 15.0 (Fig. 5). The values of bond lengths and bond angles as per the 3D structure for ligand and Co(II) complex (**1**) along with the actual ones are given in Tables S1-S3. In view of the hexacoordination of complex (**1**) (*vide* analytical and spectral studies), the molecular modelling of Co(II) complex (**1**) with two water molecules at the axial position trans to each other and the (N,N)-donor based Schiff's base ligand in *cis*-arrangement to the (O,O) confirming its octahedral structure. By comparing the values of bond lengths of two C=N and two C-O of imine and naphthyl groups of ligand to its counterpart of Co(II) complex, it is notice that the change of the two C=N and the two CO of imine and naphthyl groups bond lengths of ligand from (1.269, 1.264) Å to (1.284, 1.295) Å in complex and from (1.361, 1.366) Å in ligand to (1.487, 1.696) Å in complex, respectively by coordination with Co(II) ion indicating that, the ligand coordinates with metal ion through two imine -C=N and two naphthyl oxygens ,acting as tetradentate one. Moreover, the bond angles in the coordination sphere of Co(II) complex was found near to the perpendicular values [50]. However, a few values of optimal bond lengths /angles were lost, this may be attributed to the limitations of the software, which was observed in modelling of other systems [51]. In most of the previous studies, the calculated bond angles and lengths are near to the optimal values [51,52]. Consequently, the proposed structure of the Co(II) complex (**1**) and other complexes are acceptable.

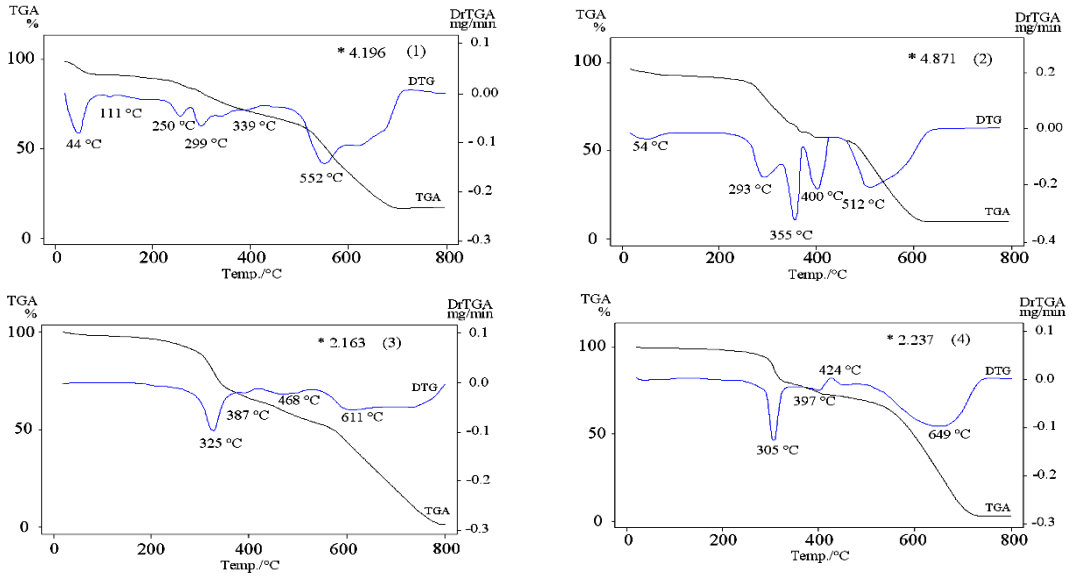

Fig. 4: TG/DTG curve of complexes (**1**-**4**)

Table 3: Thermal data of ligand H_2L and its metal complexes

	Compound	Temperature range/ (°C) DTG	Temperature range/ (°C) TGA	Mass loss % Calc.	Mass loss % (F.)	$(T_d)^a$	Leaving species
		-	28-174	-	-		Steady part
	H_2L	307,414	174-512	62.44	(62.56)	174	-Loss of naphthol, azomethine, benzene ring, 2amide groups, pyridine ring moieties($C_{24}H_{17}N_4O_3$)
		576,645	512-799	37.56	(37.44)		-Loss of benzene ring, naphthol ($C_{17}H_{12}NO$)
1	$[Co(L)(H_2O)_2].3H_2O$	44	28-116	6.72	(6.60)	220	-Loss of 3 mole of lattice water
		250,299,339 552	220-488	25.56	(24.99)		- Loss of 2 mole of coordinated water, naphthol, azomethine moieties ($C_{11}H_{11}NO_3$)
			488-799	49.32	(49.41)		-Loss of benzene ring, 2 amide groups, pyridine ring, azomethine, naphthol moieties ($C_{24}H_{17}N_4O_2$)
			799	18.40	(19.00)[b]		≡CoO+6C
2	$[Ni(L)(H_2O)_2].1½H_2O$	54	30-110	3.48	(3.28)		-Loss of 1.5 mole of lattice water
		293,355,400 512	232-432	36.12	(36.43)	232	- Loss of 2 mole of coordinated water, naphthol, azomethine, benzene ring ($C_{17}H_{14}NO_3$)
			432-650	52.79	(52.51)		≡ Ni
			650	7.61	(7.78)[b]		
3	[Cu(L)]	-	30-193	-	-		-Steady part
		325,387,468 611	193-576	50.94	(50.0)	193	-Loss of naphthol, azomethine, benzene ring, amide group, pyridine moieties ($C_{23}H_{15}N_3O_2$)
			576-799	40.20	(41.30)		-Loss of amide group, benzene ring, azomethine, naphthol moieties($C_{18}H_{12}N_2O_2$)
			799	8.86	(8.70)[b]		≡Cu
4	$[Cu(H_2L)(OH)Br]$	-	30-222	-	-		-Steady part
		305,397,424 649	222-520	32.74	(32.94)	222	- Loss of hydroxy, 0.5 mole Br_2 gas, naphthol, azomethine, ($C_{11}H_9NO_2$) moieties
			520-750	59.47	(60.01)		-Loss of benzene ring, 2 amide groups, pyridine, azomethine, naphthol moieties($C_{30}H_{21}N_4O_3$)
			750	7.79	(7.05)[b]		≡Cu

[a]: initial temperature of the decomposition; [b]: final product percent

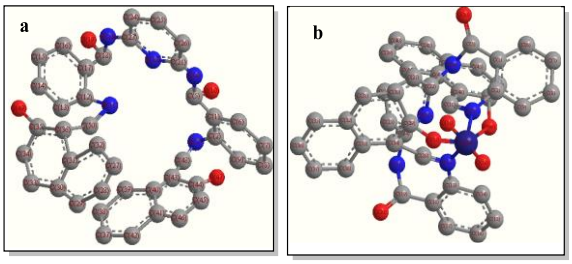

Fig. 5: Optimized geometry of: a) Schiff's base ligand and b) $[Co(L)(H_2O)_2].3H_2O$ complex(**1**).

3.6. Powder X-ray diffraction analysis

The growth of single crystals of the metal complexes was failed. So, XRD of the current ligand and its copper(II) complexes in powder samples has been carried out for further structural information [53]. The X-ray diffraction patterns of the ligand and its Cu(II) complexes **(3,4)** are shown in Figs. 6,7,8. Comparing XRD pattern of the ligand with that of its complexes (**3,4**) indicates that the relative intensities (I/I^0) and interplanar spacing d (A^0) were different, which could be related to the complexation. Moreover, the XRD patterns of [Cu(L)] **(3)** and $[Cu(H_2L)(OH)Br]$ (**4**) showed sharp peaks indicating to their crystalline nature.

The average crystallite size (D) was calculated from the sharpest peaks using Debye-Sherrer's formula [54, 55].

$$D = 0.9\lambda/\beta Cos\theta$$

Where (D) is the crystallite size in nm, λ is the wavelength (CuK_α) of X-ray, θ is Bragg diffraction angle and β-full width at half maximum (FWHM). The ligand, complexes (**3**) and (**4**) have an average crystallite size of 13.56, 20.1 and 24.95 nm, respectively, suggesting that the compounds are in nanometer range [53, 54, 56]. The data of X-ray diffraction as 2θ relative intensities and d-spacing are listed in Table S4. From the value of (D), we can compute the dislocation density (δ) value of studied compounds which indicates the number of dislocation lines per unit area of the crystal. From value of average crystallite size (D), the value of (δ) is calculated from the equation [53]:

$$\delta=1/(D)^2$$

The calculated value of (δ) was 0.00543, 0.00247 and 0.00160 nm-2 for ligand, complex (**3**) and (**4**), respectively. The difference of calculated value of (D) and (δ) for complexes **(3,4)** compared to those of the ligand is another evidence about complex formation.

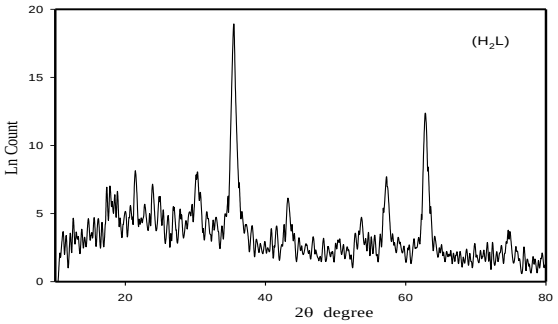

Fig. 6: X- ray powder diffraction patterns of ligand (H_2L).

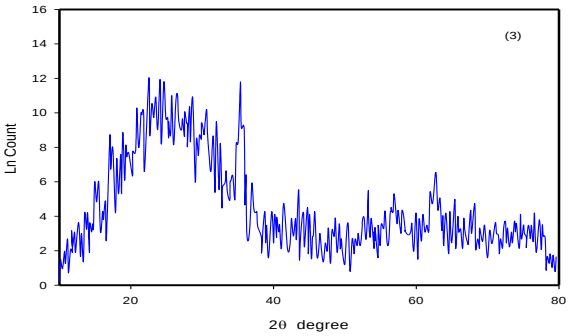

Fig. 7: X -ray powder diffraction patterns of [Cu(L)] (**3**).

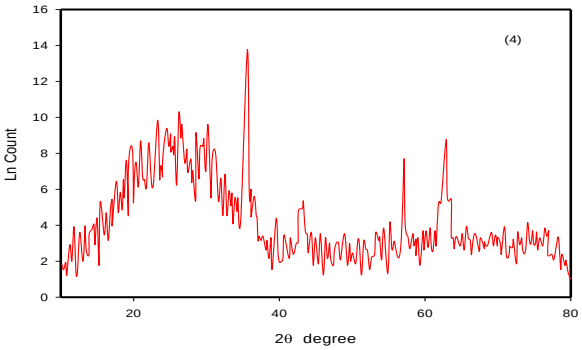

Fig. 8: X- ray powder diffraction patterns of $[Cu(H_2L)(OH)Br]$ (**4**).

Based on the above analytical, spectral, thermal, XRD and 3D molecular modelling studies, it is confirmed that the synthesized Schiff's base complexes (**1,2**) have an octahedral structure, while complexes (**3,4**) have square planar geometry. The suggested structures of the obtained complexes are given in Fig. 9.

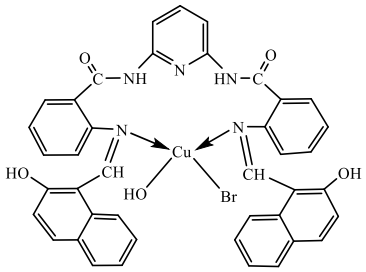

(4)

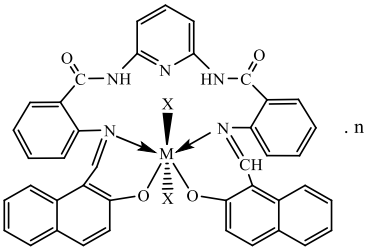

No.	M	x	n
(1)	Co(II)	H_2O	$3H_2O$
(2)	Ni(II)	H_2O	$1½H_2O$
(3)	Cu(II)	nil	nil

Fig. 9: Suggested structure of complexes.

3.7. In vitro antioxidant screening

In vitro antioxidant screening of the current compounds has been examined by 2,2-diphenyl-1-picryl hydrazyl (DPPH) free radical scavenging method using (Ascorbic acid) as standard. 2,2-diphenyl-1-picryl hydrazyl (DPPH) radical reacts with antioxidant compound as described (Scheme 2). The results were compared with those of standard antioxidant (Ascorbic acid). The percentage radical scavenging activity of the synthesized compounds

(Fig. 10) has been carried out at different concentrations (100,150, 200 μg mL^{-1}) and tabulated in Table 4. The DPPH scavenging activity was expressed as IC_{50}, the effective concentration at which 50% of the radicals were scavenged, have been computed to assess the antioxidant activities. A lower IC_{50} value indicates higher antioxidant activity. IC_{50} values lower than 10 mg/mL imply effective antioxidant activity [57].

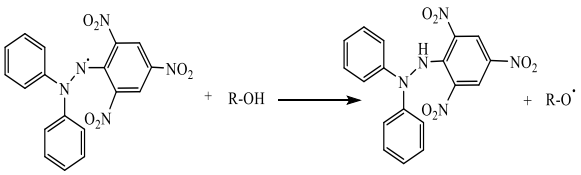

DPPH (Purple)
R-OH : Antioxdant compound
DPPH : 2,2-diphenyl-1-picrylhydrazyl

DPPH:H (Colorless)

Scheme 2: Proposed mechanism for DPPH scavenging activity with antioxidant compound.

Table 4: Inhibition% and IC50 (μg mL-1)a values of ligand and its metal complexes.

No.	Compound	Inhibition% (μg mL) 100	150	200	IC_{50} (μg mL^{-1})[a]
	H_2L	36.96	59.55	60.29	142.46
1	$[Co(L)(H_2O)_2].3H_2O$	10.68	25.05	29.21	345.37
2	$[Ni(L)(H_2O)_2].1½H_2O$	21.78	37.08	40.90	228.15
3	[Cu(L)]	16.21	29.64	33.03	248.33
4	$[Cu(H_2L)(OH)Br]$	23.68	42.64	46.03	198.27
	Ascorbic acid	35.96	58.55	59.29	144.56

[a]:(IC_{50}) the effective concentration at which 50% of the radicals were scavenged as compared to control untreated cells (μg mL^{-1}).

From the obtained results, the ligand (IC_{50} = 142.46 μg mL^{-1}) showed good activity better than ascorbic acid (IC_{50}= 144.56 μg mL^{-1}) this is due to the hydrogen donating power to DPPH complex. Cu(II)(**4**), Ni(II)(**2**) displayed moderate activity compared with the standard. The free radical scavenging activity of the studied compounds depend on structural factors as presence of naphtholic -OH, type and geometry of metal ions [58]. The order of IC_{50} values of ligand and its metal(II) complexes was as follows; H_2L > Ascorbic acid > Cu(II)(**4**) > Ni(II)(**2**) > Cu(II)(**3**) > Co(II)(**1**).

From Table 4, it is observed that, the inhibitory effect of the studied compound is depended on concentration. Suppression ratio increases with increasing sample concentration in the range tested [59].

3.8. In vitro antimicrobial property

The current Schiff's base and its metal complexes were tested for their antibacterial property against *(Staphylococcus aureus*) and (*Escherichia coli*) and for their antifungal property against (*Aspergillus flavus* and *Candida albicans*). From the obtained data depicted in Fig. 11 and tabulated in Table S5, and from photographs of antibacterial screening (Figs. S1 and S2) the following results are outlined:

- All the compounds showed a moderate activity against the bacterial strains *E. coli* and *S. aureus*, except for Cu(II) **(3)** which is inactive against the both types of bacteria and Cu(II)**(4)** which is inactive against *E. coli*.
- It is noticed that the studied complexes were more active against Gram- positive than Gram-negative bacteria.

- All the compounds are found to have no biological activity against both types of antifungal, except for ligand, that have activity against *C. albicans*.
- The obtained data indicated that the antibacterial activity is increased upon complexation except for Cu(II)(**4**) against *S. aureus* and Ni(II) complex **(2)** against *E. coli*. These results can be interpretated on view of Overtones concept and the Tweedy's chelation theory [21, 39, 60].
- Complexes with negative results indicated its inability to diffuse into the bacteria cell membrane. Some significant factors play an important role in deciding the potency of an antimicrobial agent, such as pharmacokinetic and steric factors, presence of moiety as azomethine linkage, the type of the metal ion, solubility, dipole moment and conductivity influenced by metal ion [61-64]. Further modification and/or using higher sample concentrations may improve this antimicrobial activity.

On chelation, the lipophilic nature of the coordinated metal atom increased and hence increases the liposolubility character of the complexes which subsequently favouring its permeation through the lipid layer of cell membrane. Also, cell wall structure of bacteria influences on the antimicrobial activity of the compounds because the cell wall is essential to the survival of bacteria. The differences in cell wall structure between Gram negative bacteria and Gram-positive bacteria can produce differences in the antibacterial susceptibility [35, 39, 60].

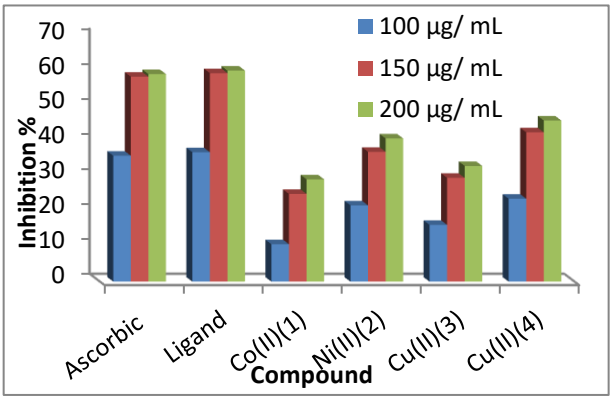

Fig. 10: In vitro antioxidant screening of all compounds by DPPH· assay at 100, 150 and 200 µg mL-1.

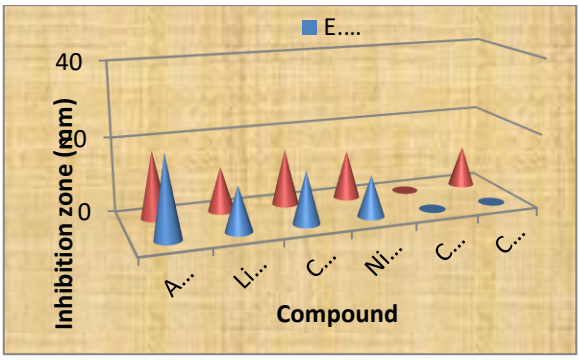

Fig. 11: Graphical representation of antibacterial screening of compounds with standard (Ampicillin) at 10 mg mL^{-1}.

4. Conclusions

In this study, new tetradentate Schiff base ligand and its complexes were prepared and assigned by microanalyses, molar conductivity, magnetic data, spectral (UV-Visible, EPR, ^{1}H NMR, MS, IR), XRD, thermal studies and 3D molecular modeling. Six coordinated structure has been assigned for the isostructural Co(II), Ni(II) complexes and square planar for Cu(II) complexes. The results of antioxidant activity of all synthesized compounds showed that the ligand possesses excellent activity even better than the reference (Ascorbic acid) and compound (4) was found to be the most potent one. *In vitro* results of antimicrobial property imply that most metal complexes are more active than their free ligand.

5. Conflicts of Interest:

The authors declare no conflict of interest.

6. Formatting of funding sources

This research received no external funding.

7. References

1. K. Mohammadi, M. Rastegari, New tetradentate Schiff bases of 2,2-dimethyl-1,3-diaminopropane and acetylacetone derivatives and their vanadyl complexes. Spectrochim. Acta A. **97**,711-716 (2012).
2. S. Roy, S. Chattopadhyay, Mono, di and trinuclear photo-luminescent cadmium(II) complexes with N_2O and N_2O_2 donor salicylidimine Schiff bases: Synthesis, structure and self-assembly. Inorg. Chim. Acta. **433**,72-77 (2015).
3. K. Mohammadi, S. S. Azad, A. Amoozegar, New tetradentate Schiff bases of 2-amino-3,5-dibromobenzaldehyde with aliphatic diamines and

their metal complexes: Synthesis, characterization and thermal stability. Spectrochim. Acta A. **146**, 221-227 (2015).

4. N. Sarkar, P. K. Bhaumik, S. Chattopadhyay, Manganese(III) complexes with tetradentate salicylaldimine Schiff bases: Synthesis, structure, self-assembly and catalase activity. Polyhedron **115**, 37- 46 (2016).

5. B. S. Creaven, B. Duff, D. A. Egan, K. Kavanagh, G. Rosair, V. R. Thangella, M. Walsh, Anticancer and antifungal activity of copper(II) complexes of quinolin-2(1H)-one-derived Schiff bases. Inorg. Chim. Acta. **363**, 4048-4058 (2010).

6. H.A. El-Boraey, R.M. Abdel-Rahman, E. M. Atia, K. H. Hilmy, Spectroscopic, thermal and toxicity studies of some 2-amino -3- cyano-1, 5–diphenylpyrrole containing Schiff base copper (II) complexes, Cent. Eur. J. Chem. **8**(4), 820-833 (2010).

7. H.A. El-Boraey, M.A. Abdel-Hakeem Facile synthesis, spectral, EPR, XRD and antimicrobial screening of some γ- irradiated N', N'''-(1E, 2E)-1,2-diphenylethane-1,2-diylidene)bis(2aminobenzohydrazide) metal complexes. J Mol Struct **1211**, 128086 (2020).

8. O. A. EL-Gammal, H. Alshater, H. A. El-Boraey, Schiff base metal complexes of 4-methyl-1H-indol-3-carbaldehyde derivative as a series of potential antioxidants and antimicrobial: Synthesis, spectroscopic characterization and 3D molecular modelling, J. Mol. Struct.1195 (2019) 220-230.

9. D. Bandyopadhyay, M. Layek, M. Fleck, R. Saha, C. Rizzoli, Synthesis, crystal structure and antibacterial activity of azido complexes of cobalt(III) containing heteroaromatic Schiff bases. Inorg. Chim. Acta. **461**, 174-182 (2017).

10. A. A. Abdel Aziz, I. H. A Badr, I. S. A. El-Sayed, Synthesis, spectroscopic, photoluminescence properties and biological evaluation of novel Zn(II) and Al(III) complexes of NOON tetradentate Schiff bases. Spectrochim. Acta A., **97**, 388-396 (2012).

11. O. A. El-Gammal, F. Sh. Mohamed, G. N. Rezk, A. A. El-Bindary, Structural characterization and biological activity of a new metal complexes based of Schiff base. J. Mol. Liq. **330,** 115522 (2021).

12. L. H. Abdel-Rahman, N. M. Ismail, M. Ismael, A. M. Abu-Dief, E.A. Ahmed, Synthesis, characterization, DFT calculations and biological studies of Mn(II), Fe(II), Co(II) and Cd(II) complexes based on a tetradentate ONNO donor Schiff base ligand. J. Mol. Struct. **1134**, 851-862 (2017).

13. S. Sukkur Saleem, M. Sankarganesh, P. Adwin Jose, J. Dhaveethu Raja, Design, synthesis, antioxidant, antimicrobial, DNA binding and molecular docking studies of morpholine based Schiff base ligand and its metal (II) complexes. Inorg. Chem. Commun. **124** 108396 (2021).

14. K. P. Rakesh, H. M. Manukumar, D. C. Gowda, Schiff's bases of quinazolinone derivatives: Synthesis and SAR studies of a novel series of potential anti-inflammatory and antioxidants. Bioorg. Med. Chem. Lett. **25**, 1072-1077 (2015).

15. K. Amimoto, T. J. Kawato, Photochromism of organic compounds in the crystal state. Photochem. Photobiol C Photochem. Rev. **6**, 207-226 (2005).

16. E. Hadjoudis, A. Rontoyianni, K. Ambroziak, T. Dziembowska, I. M. Mavridis, Photochromism and thermochromism of solid trans-*N*,*N'*-bis-(salicylidene)-1,2- cyclohexanediamines and trans-*N*, *N'*-bis-(2-hydroxy-naphylidene)-1,2-cyclohexanediamine. J. Photochem. Photobiol. A. **162**, 521-530 (2004).

17. D. Sek, M. Siwy, K. Bijak, M. Filapek, G. Malecki, E. M. Nowak, J. Sanetra, A. J. Jedryka, K. Laba, M. I. Lapkowsk, E. S. Balcerzak, Optical and electrochemical properties of novel thermally stable Schiff bases bearing naphthalene unit. J. Electroanal. Chem. **751**,128-136 (2015).

18. P. Sılku, S. Özkınalı, Z. Öztürk, A. Asan, D. A. J. Köse, Synthesis of novel Schiff bases containing acryloyl moiety and the investigation of spectroscopic and electrochemical properties. J. Mol. Struct. **1116**, 72-83 (2016).

19. T. K. Chaitra, K. N. S. Mohana, H. Ch. Tandon, Thermodynamic, electrochemical and quantum chemical evaluation of some triazole Schiff bases as mild steel corrosion inhibitors in acid media. J. Mol. Liq. **211**, 1026-1038 (2015).

20. P. Singh, M. A. Quraishi, Corrosion inhibition of mild steel using novel bis Schiff's bases as corrosion inhibitor: Electrochemical and surface measurement. Measurement **86**, 114-124 **(**2016).

21. P. Subbaraj, A. Ramu, N. Raman, J. Dharmaraja, Synthesis, characterization, DNA interaction and pharmacological studies of substituted benzophenone derived Schiff base metal(II) complexes. J. Saud. Chem. Soc. **19**, 207-216 (2015).

22. M. A. Mahmoud, S. A. Zaitone, A. M. Ammar, S. A. Sallam, Synthesis, structure and antidiabetic activity of chromium(III) complexes of metformin Schiff-bases. J. Mol. Struct. **1108**, 60-70 (2016).

23. Beena, D. Kumar, D. S. Rawat, Synthesis and antioxidant activity of thymol and carvacrol based Schiff bases. Bioorg. Med. Chem. Lett. **23**, 641-645(2013).

24. S. Yadav, M. Ahmad, K. S. Siddiqi, Metal-ion directed synthesis of N_2O_2 type chelate complexes

of Ni(II), Cu(II) and Zn(II): Spectral, thermal and single crystal studies. Spectrochim. Acta A., **98**, 240-246 (2012).

25 J. Bassett, R. C. Denney, G. H. Jeffery, J. Mendham, Vogel's Textbook of quantitative inorganic analysis including elementary instrumental analysis, 4th edition, Longman Group, London, 316-322 (1978).

26. T. S. West, Complexometry with EDTA and Related Reagents, 3rd edn, DBH Ltd., Pools West TS, (1969) Complexometry with EDTA and Related Reagents, 3rd edn, DBH Ltd., Pools

27. H. A. El-Boraey, A. A. Serag El-Din, Transition metal complexes of a new 15-membered [N_5] penta-azamacrocyclic ligand with their spectral and anticancer studies. Spectrochim. Acta A. **132**, 663-671(2014).

28. R. Amarowicz, R. B. Pegg, P.R. Moghaddam, B. Barl, J.A. Weil, Free-radical scavenging capacity and antioxidant activity of selected plant species from the Canadian prairies. Food Chem. **84**, 551-562 (2004).

29. M. S. Blois, Antioxdant determination by the use of a stable free radical. Nature. **181**,1199-1200 (1958).

30. A.W. Bauer, W.M. Kirby, C. Sherris, M. Turck, Antibiotic susceptibility testing by a standardized single disk method. Am. J. Clin. Pathol. **45**(4), 493-496 (1966).

31. W. J. Geary, The use of conductivity measurements in organic solvents for the characterization of coordination compounds. Coord. Chem. Rev**. 7**, 81-122 (1971).

32. H. A. El-Boraey, A. A. El-Gokha, I. El-Sayed, M. A. Azzam, Transition metal complexes of α-aminophosphonates Part I: synthesis, spectroscopic characterization, and in vitro anticancer activity of copper(II) complexes of α-aminophosphonates. Med. Chem. Res. **24**, 2142-2153 (2015).

33. R. K. Jain, A. P. Mishra, Microwave synthesis, spectral, thermal, 3D molecular modeling analysis and antimicrobial activities of some transition metal complexes of Schiff bases derived from 5-bromosalicylaldehyde J. Saud. Chem. Soc. **20**,127-137 (2016).

34. S. A. Patil, S. N. Unki, A. D. Kulkarni, V. H. Naik, B. S. Badami, Co(II), Ni(II) and Cu(II) Complexes with coumarin-8-yl Schiff-bases: Spectroscopic, in vitro antimicrobial, DNA cleavage and fluorescence studies. Spectrochim. Acta A. **79**,1128-1136 (2011).

35. O. A. El-Gammal, M. M. Bekheit, S. A. El-Brashy, Synthesis, characterization and in vitro antimicrobial studies of Co(II), Ni(II) and Cu(II) complexes derived from macrocyclic compartmental ligand. Spectrochim. Acta A. **137**, 207-219 (2015).

36. H. A. El-Boraey, Structural and thermal studies of some aroylhydrazone Schiff's bases-transition metal complexes. J. Therm. Anal. Calorim., **81**, 339-46 (2005).

37. S. Kumar, A. Hansda, A. Chandra, A. Kumar, M. Kumar, M. Sithambaresan, S. Haque Faizi, V. Kumar, R. P. John, Co (II), Ni(II), Cu(II) and Zn(II) complexes of acenaphthoquinone 3- (4-benzylpiperidyl) thiosemicarbazone: Synthesis, structural, electrochemical and antibacterial studies. Polyhedron **134**, 11-21 (2017).

38. M. Shakir, A. Abbasi, M. Azam, A.U. Khan, Synthesis, spectroscopic studies and crystal Structure of the Schiff base ligand L derived from condensation of 2-thiophenecarboxaldehyde and 3,3-diaminobenzidine and its complexes with Co(II), Ni(II), Cu(II), Cd(II) and Hg(II): Comparative DNA binding studies of L and its Co(II), Ni(II) and Cu(II) complexes. Spectrochim. Acta A. **79**, 866-1875 (2011).

39. M. M. Ibrahim, G. A. M. Mersal, A. M. Ramadan, S. A. El- Shazly, M. A. Amin, Spectroscopic, electrochemical, catechol oxidase and catalase like activities of new Copper(II) tweezersof benzimidazole incorporating amino acid moieties. J. Electrochem. Sci. **9**, 5298-5314 (2014).

40. A. Z. El-Sonbati, M. A. Diab, A. A. El-Bindary, M. I. Abou-Dobara, H. A. Seyam, Supramolecular coordination and antimicrobial activities of constructed mixed ligand complexes, Spectrochim. Acta A. **104**, 213-221 (2013).

41. A. A. Osowole, E. Akpan, Synthesis, spectroscopic characterization, *in vitro* anticancer and antimicrobial activities of some metal(II) complexes of 3-{4, 6- dimethoxy pyrimidinyl) iminomethyl naphthalen-2-ol, J. Euro. J. Appl. Sci. **4**(1),14-20 (2012).

42. H. A El-Boraey, A. A. Serag El-Din, I. El-Sayed, New complexes with 19-membered pyridine-based macrocycle ligand: Synthesis, characterization, thermal and in vitro anticancer activity. J. Therm. Anal. Calorim. **129**, 1243-1253 (2017).

43. H. A. El-Boraey, O. A. El-Gammal, Macrocyclic Cu(II) and Pd(II) complexes with new 16-membered tetradentate [N_4] ligand: synthesis, characterization, 3D molecular modelling and in vitro anticancer and antimicrobial activities. J. Incl. Phenom. Macrocycl. Chem. **90**,123-134 (2018).

44. M. Shebl, S. M. E. Khalil, F. S. Al-Gohani, Preparation, spectral characterization and antimicrobial activity of binary and ternary Fe(III), Co(II), Ni(II), Cu(II), Zn(II), Ce(III) and UO_2(VI) complexes of a thiocarbohydrazone ligand. J. Mol. Struct., **980**, 78-87 (2010).

45. D. Kivelson, R. Neiman, ESR studies on the bonding in copper complexes. J. Chem. Phys. **35**,149-155 (1961).

46. B. J. Hathaway, D. E. Billing, Billing DE, The electronic properties and stereochemistry of mononuclear complexes of the copper(II) ion. Coord. Chem. Rev. **5**, 143-207 (1970).

47. H. A. El-Boraey, F. A. El-Saied, S. A. Aly, UO_2(VI), Sn(IV), Th(IV) and Li(I) complexes of 4-azomalononitrile antipyrine, synthesis, characterization and thermal studies. J. Therm. Anal. Calorim. **96**, 599-606 (2009).

48. H. A. El-Boraey, A. I. Mansour, Synthesis, spectral and gamma ray irradiation studies on metal complexes of N, N'-naphthalene-1,8-diylbis(2-aminobenzamide). Inorg. Nano-met. Chem. **48**, 8-15 (2018).

49. A. M. Donia, H. A. El- Boraey, Thermal investigation of cobalt, nickel and copper complexes with 8-aminoquinoline correlation between thermal stability and crystal field splitting energy. J. Therm. Anal. **48**, 1325-1336 (1997).

50. H. L. Singh, J. Singh, Synthesis, spectral, 3D molecular modelling and antibacterial studies of dibutyltin(IV) Schiff base complexes derived from substituted isatin and amino acids. Natural. Sci. **4**, 170-178 (2012).

51. R. C. Maurya, J. Chourasia, P. Sharma, Bis(o-vanillin)benzidine(o-v_2bzH_2) as a binucleating ligand: Synthesis, characterization and 3D molecular modeling and analysis of some binuclear complexes of (o-v_2bzH_2) with copper(II), nickel(II), cobalt(II), manganese(II), zinc(II), samarium(III) and dioxouranium(VI). Indian. J. Chem. Sect. A. **47**, 517-528 (2008).

52. R. C. Maurya, S. Jham, S. Roy, J. Chourasia, A. K. Sharma, P. Vishwakarma, Synthesis, characterization, and 3D-molecular modelling and analysis of some copper(II) chelates in O,N-donor coordination pattern involving Schiff bases derived from 4-butyryl-3-methyl-1-phenyl-2-pyrazolin-5-one and some sulfa drugs. Arab. J. Chem. **8**,143-154 (2015).

53. H.F. Abd El-Halim, G.G. Mohamed, M.N. Anwar, Antimicrobial and anticancer activities of Schiff base ligand and its transition metal mixed ligand complexes with heterocyclic base. Appl. Organometal. Chem. **32**, (1) 3899 (2018).

54. R.S. Joseyphus, M.S. Nair, Synthesis, characterization and biological studies of some Co(II), Ni(II) and Cu(II) complexes derived from indole-3-carboxaldehyde and glycylglycine as Schiff base ligand. Arab. J. Chem. **3**(4), 195-204 (2010).

55. D. Arish, M. S. Nair, Synthesis of some Schiff base metal complexes involving para substituted aromatic aldehydes and glycylglycine: Spectral, electrochemical, thermal and surface morphology studies. J. Mol. Struct., **983**,112-121 (2010).

56. S. Aly, H.A. El-Boraey, Effect of gamma irradiation on spectral, XRD, SEM, DNA binding, molecular modelling and antibacterial property of some (Z)N-(furan-2-yl)methylene)-2-(phenylamino)acetohydrazide metal(II) complexes. J. Mol. Struct. **1185**, 323-332 (2019).

57. Y. L. Lee, M. T. Yen, J. L. Mau, Antioxidant properties of various extracts from Hypsizigus marmoreu. Food Chem. **104**, 1-9 (2007).

58. H.A. El-Boraey, M.A. El-Salamony, Transition metal complexes with polydentate ligand: synthesis, characterization, 3D molecular modelling, anticancer, antioxidant and antibacterial evaluation. J. Inorg. Organomet. Polymer **29**, 684-700 (2019).

59. A. M. Ajlouni, Q. A. Salem, Z. A. Taha, A. K. Hijazi, W. A. Momani, Synthesis, characterization, biological activities and luminescent properties of lanthanide complexes with [2-thiophenecarboxylic acid, 2-(2-pyridinylmethylene) hydrazide] Schiff bases ligand. J. Rare Earths. **34**(10), 986-993 (2016).

60. B. G. Tweedy, Plant extracts with metal ions as potential antimicrobial agents. Phytopathology **55**, 910-918 (1964).

61. M. SÖnmez, Ç. Metin, I. Berber, Synthesis, spectroscopic and biological studies on the new symmetric Schiff base derived from 2,6-diformyl-4-methylphenol with N-aminopyrimidine. Eur. J. Med. Chem. **45**, 1935-1940 (2010).

62. D. P. Singh, V. Grover, P. Rathi, K. Jain, Trivalent transition metal complexes derived from carbohydrazide and dimedone. Arab. J. Chem. **10**, S1795-S1801 (2013).

63. H. A. El-Boraey, M. A. El-Salamony, A. A. Hathout, Macrocyclic [N_5] transition metal complexes: synthesis, characterization and biological activities. J. Incl. Phenom. Macrocycl. Chem. **86**,153-166 (2016).

64. H. Alshater, H. A. El-Boraey, A. M.A. Homoda, O. A. EL-Gammal, Improving the surface morphology and crystallite size of isonicotinohydrazide based binuclear Cr(III), Zn(II) and Sn(IV) complexes after irradiation with γ -rays. J. Mol. Struct. **1232**, 129985 (2021).